Bitlis Eren Üniversitesi Fen Bilimleri Dergisi
BİTLİS EREN UNIVERSITY JOURNAL OF SCIENCE
ISSN: 2147-3129/e-ISSN: 2147-3188
VOLUME: 12 NO: 2 PAGE: 445-454 YEAR: 2023
DOI:10.17798/bitlisfen.1237388

# Performance Optimization of Auxetic Structures on Energy Absorption of Cylindrical Sandwich Using Taguchi and ANOVA Methods

Onur KAYA[1*], Ali Husnu BADEMLIOGLU[2], Cihan KABOGLU[3]

[1]*ERMETAL Automotive, R&D Center, Bursa/Turkey*
[2]*Bursa Technical University, Faculty of Engineering and Natural Sciences, Department of Mechanical Engineering, Bursa/Turkey*
[3]*Bursa Technical University, Faculty of Engineering and Natural Sciences, Department of Metallurgical and Materials Engineering, Bursa/Turkey*

*(ORCID: 0000-0002-8010-6707) (ORCID: 0000-0001-6944-4900) (ORCID: 0000-0002-6249-0565)*

**Keywords:** Auxetic, Energy Absorption, Taguchi, ANOVA

**Abstract**

High engineering requirements for shock absorbers have increased interest in auxetic materials, which have higher specific energy absorption performance compared to conventional solid absorbers. In the last decade, many optimization studies have been conducted to improve the energy absorption performance of auxetic tubular structures. Most studies focused on adding inner and outer shells to thin-walled auxetic tubular absorbers with different types of lattice structures to enhance the energy absorption of the cylindrical sandwiches. There are limited studies on thicker-walled auxetic tubes and their related shell thicknesses to optimize performance. In this study, the thickness of the thicker-walled auxetic core thickness (1.2 mm, 1.6 mm, and 2 mm), shell thickness (16 mm, 20 mm, and 24 mm), and auxetic lattice structure (Re-Entrant Circular, SiliComb, and ArrowHead) were optimized to improve the specific energy absorption of cylindrical sandwiches. The Taguchi method was used to determine the optimum parameters for cylindrical sandwiches. In addition, the effect ratio of the parameters on the specific energy absorption was investigated using the ANOVA method. The energy absorption properties of the cylindrical sandwiches were determined using the drop-weight test. The highest specific energy absorption was obtained using a shell thickness of 1.2 mm and a core thickness of 16 mm using a SiliComb lattice. It was determined that the lattice geometry was the most effective parameter for the specific energy absorption of cylindrical sandwiches, with an effect rate of 61.62%.

## 1. Introduction

In recent years, developments in the fields of design and technology have led to high engineering requirements. A challenge over a new lighter material without any strength or stiffness loss has been started to meet this demand. Alternatively, new structural materials that have a negative Poisson's ratio may be of interest. "Auxetic" refers to the behaviour of materials that have a negative Poisson's ratio. When auxetic materials are stretched in the longitudinal direction, they elongate transversely, in contrast to conventional materials [1]. Along with superior indentation resistance, shearing resistance, and fracture toughness, auxetic materials also exhibit unique energy absorption compared to conventional materials [2].

The absorption behaviour of materials reduces the amount of energy transferred to the passengers of the vehicle in the event of a collision. Consequently, energy absorption performance is desired to be higher [3]. The energy absorption

*Corresponding author: o.kaya@ermetal.com
*Received: 03.02.2023, Accepted: 16.06.2023*

capacity of a material is directly related to its mass. Massive materials naturally absorb more energy. Specific Energy Absorption (SEA) enables the comparison of materials independent of mass. SEA refers to the energy absorption capacity of a material per mass. Auxetic materials have improved SEA compared to conventional materials [4].

Energy absorbers can basically be classified as solid or tubular. Research shows that tubular materials exhibit excellent energy absorption performance compared to solid materials under equal mass conditions [5]. Furthermore, when compared to straight tubular materials, auxetic tubular materials offer superior crashing performance [6], [7]. When the cylindrical inner and outer surfaces of the auxetic tubular material are covered with a shell, SEA increases dramatically. Guo et al. increased the SEA four times by covering the 4 mm thick auxetic tubes with 0.1 mm thick shells [8]. On the other hand, reinforcing a tubular absorber with a solid auxetic filler reduces the SEA value by about half [9]. A cylindrical sandwich consists of a tubular auxetic core with interior and exterior shells. The lattice geometry of the auxetic core, the thickness of the auxetic core, and the thickness of the shell are the essential factors influencing the SEA [10]. The lattice geometry is obtained by designing different patterns. Zhang et al., used the lattice design of tubular structures as a rotation and offset method [11]. It is possible to design a cylindrical sandwich from all auxetic lattices by the offset method. However, there is limited research on the energy absorption performance of different lattice geometries of the auxetic core, such as honeycomb, re-entrant, and Arrow-Head (AH) [8], [10], [12].

Applied compression to the energy absorbers under dynamic loading conditions indicates their crash performance. Test materials absorb the crashing energy of a free-falling load in the vertical direction or an accelerated load in the horizontal direction [7], [13]. A diagram is obtained by recording the contact force and displacement during the crash test. The absorbed energy is characterised by the area under the force-displacement plot. Experimental studies are used to determine the absorbed energy in order to enhance the material's crash performance.

Numerical methods such as FEA or experimental design methods such as Taguchi and ANOVA help to enhance the energy absorption behaviours of auxetic materials without additional experiments [14], [15]. The Taguchi design is provided to optimize the variables of the cylindrical sandwich in order to achieve SEA as a design objective. Taguchi is used to compare different factors and their effects on the absorption energy of the auxetic structures [16]. It is also used to identify the main factors that influence the compression properties and failure behaviour of the structures. Additionally, Taguchi and ANOVA allow for the optimization of the parameters to obtain the optimal combination of the variables involved in the process, as well as the calculation of the signal-to-noise (S/N) ratio. This helps to improve the accuracy and reliability of the results and the efficiency of the process. [15]

In this study, the effect of lattice geometry (Re-Entrant Circular (REC), SiliComb (SC), and Arrow-Head (AH)), core thickness (1.2 mm, 1.6 mm, and 2 mm), and shell thickness (16 mm, 20 mm, and 24 mm) on the energy absorption performance of cylindrical sandwich composites were investigated. However, the impact of these parameters on the energy absorption performance of cylindrical sandwich composites with a statistical approach has not been encountered in the literature. For this reason, the purpose of this study is to examine the parameters that present the most significant effect on the energy absorption performance of cylindrical sandwiches and determine the importance order of these parameters by utilizing Taguchi and ANOVA methods. The results obtained from the statistical analyses can be used as a guide to determine the optimum working conditions.

## 2. Material and Method

### 2.1. Tensile Test

Dog-bone shaped specimens were 3D printed using the fused deposition modelling (FDM) method to obtain the tensile properties of the ABS. The 3D printing parameters of the test specimens are shown in Table 1. The overall dimensions of the test specimen are shown in Figure 1a. The changing of the raster angle according to the position of the 3D printed material on the print bed causes anisotropy in the material. To consider the variation of tensile properties, the test specimens shown in Figure 1b were positioned in the X and Y directions separately on the print bed.

The tensile test is adequate to validate the mechanical properties of the constitutive material of the auxetic lattice [17]. Tensile tests were conducted with the Zwick/Roell Z020 universal testing machine, whose maximum load capacity is 20 kN. Three tensile tests were performed for each direction (X and Y) according to EN ISO 527-1 at a rate of 2 mm/min. A

digital extensometer measured the deformation of the specimens to obtain the strain accurately.

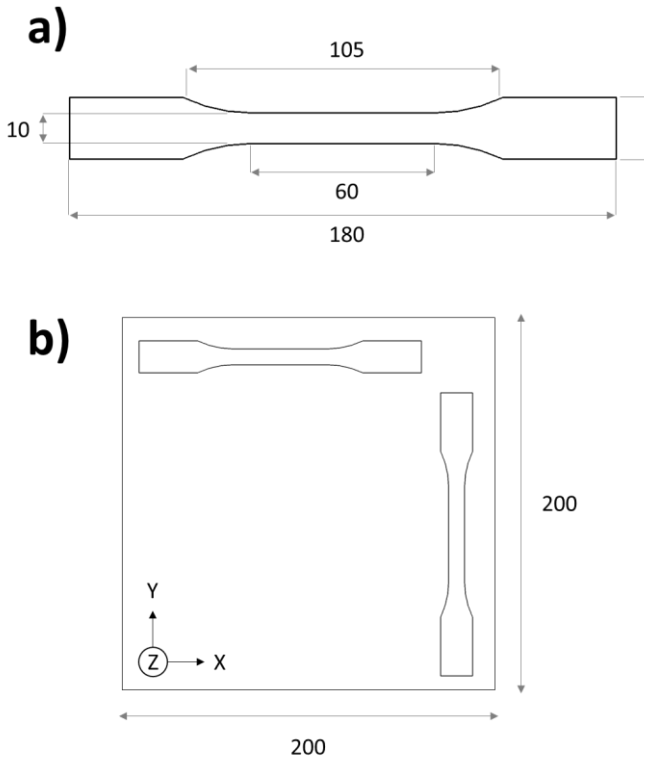


**Figure 1.** Dog-bone shaped strain test specimen a) Dimensions in 4mm thickness b)3D Printing position on Print bed. (Dimensions given in mm unit)

### 2.2. 3D Printing of Cylindrical Sandwiches

Cylindrical sandwiches were designed using SolidWorks CAD software. Auxetic lattices shown in Figure 2 (upper) were expanded in the radial direction. The auxetic core consists of aligned multi-layered lattices around a cylinder. The 3D printed cylindrical sandwich consisted of an auxetic core covered by inner and outer shells. There is limited research on the lattice geometry of the auxetic core. In the literature, the effect of geometry on the energy absorption has been investigated. Based on this research, re-entrant, honeycomb, and AH geometry were used in the study. REC is a lattice geometry that has a higher SEA in panel form than Re-entrant lattice [18]. SILICOMB (SC) is a combination of the hexagonal and re-entrant lattices which has a higher SEA than both [8]. Figure 2a, b, and c (lower) show AH, REC, and SC structured cylindrical sandwiches, respectively. Core thickness, which describes the amount of expansion in the radial direction, was 16, 20, and 24 mm. Inner and outer shells had equal thicknesses of 1.2 mm, 1.6 mm, and 2 mm. The dimensions of the lattices and sandwiches are given in Figure 2d.

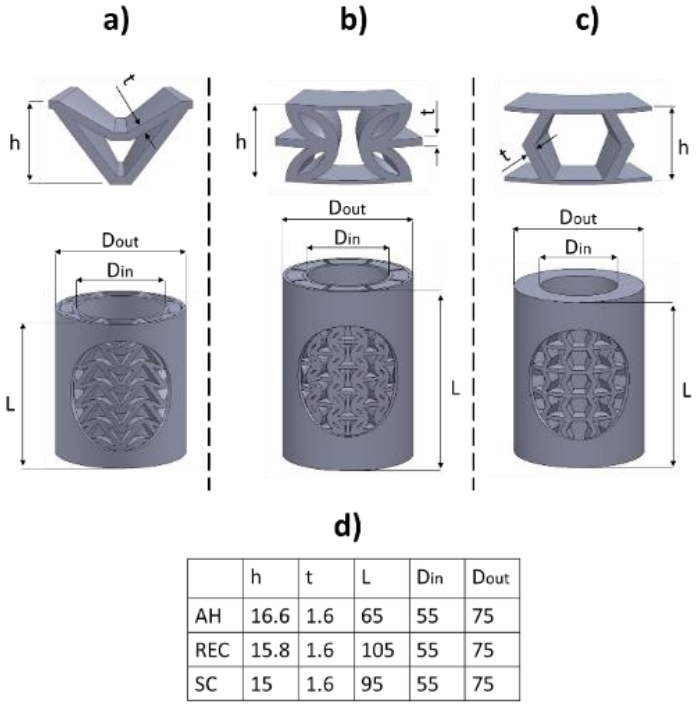


| | h | t | L | Din | Dout |
|---|---|---|---|---|---|
| AH | 16.6 | 1.6 | 65 | 55 | 75 |
| REC | 15.8 | 1.6 | 105 | 55 | 75 |
| SC | 15 | 1.6 | 95 | 55 | 75 |

**Figure 2.** Structure of sandwiches a) AH lattice b) REC lattice c) SC lattice d) Dimensions. (Dimensions given by mm unit)

Cylindrical sandwiches were 3D printed using an Ekser 3B Plus 3D printer. ESUN commercial ABS filament was used for 3D printing. The effect of 3D printing parameters on surface, dimensional, and mechanical properties is researched in detail. Compressive strength is directly related to porosity. The lower porosity causes higher compressive strength [19], [20]. Also, surface quality, dimensional accuracy, tensile strength, and residual stresses are related to layer height, built orientation, raster angle, and speed of deposition, respectively [21]. The 3D printing parameters determined by considering physical properties, especially compressive strength, are the same as the tensile test specimens shown in Table 1. The 3D printing temperature, which slightly affects the physical properties, was adjusted to 270ºC in accordance with the manufacturer's recommendation. There is no post-process such as grinding, polishing, thermal, or chemical treatment. The weights of the materials were determined by a precision scale.

**Table 1.** 3D Printing parameters of the tensile test specimens.

| Parameter | Value |
|---|---|
| Raster Angle | 30/-60º |
| Layer Height | 0.3 mm |
| Extrusion Diameter | 0.4 mm |
| Extrusion Temperature | 272ºC |
| Speed of deposition | 32 mm/s |

### 2.3. Drop Weight Tests

Analyzing an impacted weight from a drop hammer, a pendulum, or an inclined sled can identify a material's ability to absorb energy [22]. The characteristics of the impact weight influence material response. An impact weight that is liable to penetrate the material with a tip such as a hemispherical or square tip is preferred when blocking of the weight is desired. Besides, the holistic impact of the weight on the material is related to its energy transferring capacity. A flat drop hammer provides holistic impact, which distributes the energy across the lattice, whereas a hemispherical hammer provides penetration, which concentrates the energy in the centre of the lattice [23]. The holistic impact can be applied in horizontal, vertical, or inclined directions.

The drop-weight impact test is one of the common methods for the calculation of SEA [13], [14]. The transferred energy is absorbed by the deformed test material. The absorbed energy $E_a$ given in Eq. (1) is equal to the product of reaction force $F_r$ and amount of deformation $\Delta_s^f$:

$$E_a = F_r \Delta_s^f \tag{1}$$

The drop-weight impact test reveals a series of $F_r$ and $\Delta_s^f$ during the impact. Force-displacement curves are obtained by $F_r$ and $\Delta_i^s$, respectively. The area under the shadow of the force-displacement curve gives the total amount of absorbed energy $\boldsymbol{E_t}$. The SEA given in Eq. (2) is the ratio of the total amount of $\boldsymbol{E_t}$ to the mass of the specimen $\boldsymbol{m}$ that was tested.

$$\boldsymbol{SEA} = \frac{\boldsymbol{E_t}}{\boldsymbol{m}} \tag{2}$$

SEA is an indicator of the effect of parameter variations on the amount of absorbed energy for cylindrical sandwiches [8], [10], [12].

Set-up of the drop weight impact test shown in **Hata! Başvuru kaynağı bulunamadı.**a was used in this study. The set-up of the drop weight, which is shown in **Hata! Başvuru kaynağı bulunamadı.**, impacted the cylindrical sandwich. The hammerhead, which has a weight of 580 kg, indicated by number 1, was released at a height of 350 mm from the test specimen placed on the support plate indicated by number 4. Contact forces and displacement of the hammerhead were recorded by the load cell and displacement sensor, indicated by numbers 2 and 3, respectively, during the impact. **Hata! Başvuru kaynağı bulunamadı.** b and c show test specimen #1 placed in the test machine before and after the impact is applied, respectively.

Force-displacement curves are obtained from the data of the load cell and displacement sensor. The area of each slice is formed by $F_r$ and $\Delta_s^f$ is equal to $E_a$ given in equation 1. $\boldsymbol{E_t}$ or the area under the shadow of the force-displacement curve is calculated by the total amount of slices. SEA is obtained by the ratio of each $\boldsymbol{E_t}$ to mass of the related sample.

### 2.4. Taguchi Method

The Taguchi method is one of the most reliable design and optimization techniques to determine the optimal combination of different parameters for the target function. The Taguchi method provides an effective and systematic way to achieve results with far less experimentation.

In this study, it was determined that lattice geometry, shell thickness, and core thickness were target factors for the optimization of the cylindrical sandwich. Several levels of the target factors were evaluated to optimize the energy absorption performance. SEA, which was obtained by drop weight tests, was the indicator of the target factors. The design of the experiment was utilized to compare the levels of each factor to find the optimum level. A full factorial design of experiments required 27 experiments for three factors at three levels. The Taguchi method was used to optimize the target factors with fewer experiments. The orthogonal array table (L9), which requires 9 experiments, is shown in In data analysis, the results of the target functions are converted into the S/N ratio. Depending on the objective function type, three different S/N ratios are used for the calculations, i.e., the lower is the better, the higher is the better, and the nominal is the best. In this study, since the highest specific energy

absorption is the target function, the higher the better characteristic has been selected. The S/N ratios for the higher is better situation are calculated using Eq. (3):

$$S/N = -10log\left(\frac{1}{n}\sum_{i=1}^{n} y_i{}^2\right) \quad (3)$$

In this equation, $n$ indicates the number of tests (i.e., number of case) and $y_i$ defines the resulting value for the $i$th performance characteristics.

**Table 2.**

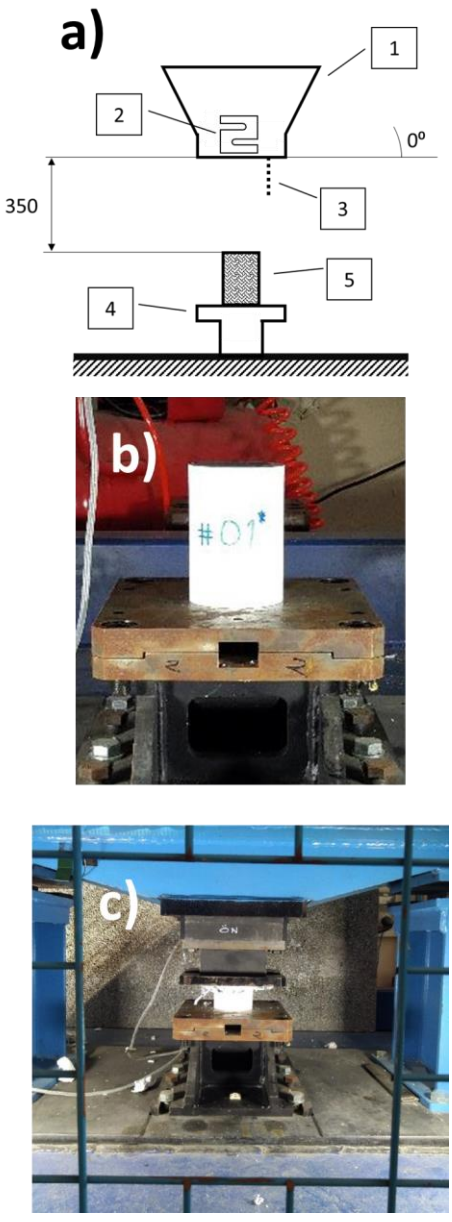


**Figure 3.** Drop weight test set-up a) schematic view (1: hammer head 2: load cell 3: displacement sensor 4: support plate 5: test specimen) b) detailed view of the test specimen #1 on the support plate c) overall view.

In data analysis, the results of the target functions are converted into the S/N ratio. Depending on the objective function type, three different S/N ratios are used for the calculations, i.e., the lower is the better, the higher is the better, and the nominal is the best. In this study, since the highest specific energy absorption is the target function, the higher the better characteristic has been selected. The S/N ratios for the higher is better situation are calculated using Eq. (3):

$$S/N = -10log\left(\frac{1}{n}\sum_{i=1}^{n} y_i{}^2\right) \quad (3)$$

In this equation, $n$ indicates the number of tests (i.e., number of case) and $y_i$ defines the resulting value for the $i$th performance characteristics.

**Table 2.** Levels and factors in accordance with the Taguchi design.

| Factor | Level 1 | Level 2 | Level 3 |
|---|---|---|---|
| **Lattice Geometry** | REC | SC | AH |
| **Shell Thickness** | 1.2 | 1.6 | 2.0 |
| **Core Thickness** | 16 | 20 | 24 |

### 2.5. ANOVA Method

ANOVA, which enables analysis with fewer experiments, compares the effect rates of factors, unlike the Taguchi method, which compares the levels of factors. The same 9 experiments from the Taguchi method were evaluated for ANOVA. SEA, which was obtained by drop weight tests, was the indicator of the target factors. Lattice geometry, shell thickness, and core thickness were the target factors to determine how much they affected the SEA. The power of each factor was represented by the contribution (P) ratio, which provides a numerical approach to compare factors. Data obtained from the drop weight test was analysed, and P values were calculated.

ANOVA is a statistical method that is utilized to determine the contribution ratios of each parameter to the response variable. By comparing the importance levels acquired from the Taguchi method, the ANOVA method can validate statistical analysis results. In the ANOVA method, contribution ratios of each parameter, degree-of-freedom (DOF), sum of

squares (SS), mean of squares (MS), and F values are calculated by the following equations:

$$F_{factor} = \frac{V_{factor}}{V_{error}} \quad (4)$$

$$V_{factor} = \frac{SS_{factor}}{DOF_{factor}} \quad (5)$$

$$DOF_{factor} = k - 1 \quad (6)$$

$$SS_{factor} = \frac{\sum \beta_{factor,i}^2}{N} - \frac{(\sum \beta_i)^2}{n} \quad (7)$$

where $F_{factor}$ is the factor's test value and is used to determine whether the term is associated with the response. $V_{factor}$ and $V_{error}$ values are the variance of the factor and error, respectively. $DOF_{factor}$ is the number of factor's degree of freedom, $SS_{factor}$ is the sum of squares due to the factor, $\beta_{factor,i}$ is the sum of the S/N ratio at the ith level of the factor, $\beta_i$ is the S/N ratio at the *i*th level of the factor, N is the repeating number of each level's factor, n is the number of tests. In these equations, "factor" represents the name of the individual factors. MS is equal to the ratio of the SS values of each parameter to the DOF of each parameter [24].

## 3. Results and Discussion

### 3.1. Tensile Tests

The ultimate tensile strength (UTS) of the 3D-printed ABS changes from 3.95 to 36.03 MPa depending on the part orientation, raster angle, and raster width [25]. Three tensile samples in each direction (X and Y) were tested. 3D printed ABS materials with 30 º and -60 º angled rasters had 30.1 and 32.27 MPa mean UTS, respectively. Table 3 shows the results of the tensile tests. A slight difference was found between the raster angles. The material used in this study with 30/-60º raster angle had a relatively high UTS compared to previous studies.

### 3.2. Drop Weight Tests

Nine drop weight tests were performed for each specimen. Force-displacement curves obtained from the drop weight tests are shown in Figure 4. Force-displacement curves had a characteristic slope depending on their lattice geometry. The force-displacement curve of the REC lattice shown in Figure 4a had a significant initial peak force at a large displacement area at the early stage of impact. A few peak forces, which do not contribute to enlarging the energy absorption area, followed the initial peak force. The force-displacement curves of the SC and AH lattices shown in Figure 4 b and c had a slightly separated initial peak force. Lots of balanced peak forces, which followed the initial peak force, kept the average force higher. SC lattice had sharper peak forces than AH lattice.

**Table 3.** Tensile properties of the ABS which constitutive material of the auxetic sandwiches.

| Specimen | UTS (N/mm$^2$) | Strength at Break (N/mm$^2$) | Elongation at Break (%) |
|---|---|---|---|
| #X1 | 29.46 | 28.71 | 1.83 |
| #X2 | 30.09 | 29.77 | 1.85 |
| #X3 | 30.75 | 30.45 | 1.96 |
| Std. Dev. | 0.65 | 0.88 | 0.07 |
| Mean X | 30.10 | 29.64 | 1.88 |
| #Y1 | 32.42 | 28.20 | 3.81 |
| #Y2 | 32.22 | 27.48 | 3.29 |
| #Y3 | 32.17 | 27.82 | 2.89 |
| Std. Dev. | 0.13 | 0.36 | 0.46 |
| Mean Y | 32.27 | 27.83 | 3.33 |

The amounts of absorbed energy were obtained from the area under the force-displacement curves for each experiment. SEA was calculated as the ratio of absorbed energy to mass. Absorbed energy and SEA values of experiments are shown in Table **4**. Considering the lattice geometry, REC had relatively high energy absorption, followed by SC and AH. SEA was too complexly distributed to explain the factors or levels related to mass. On the other hand, a clear relation wasn't found between values of absorbed energy, or SEA, without the Taguchi method or ANOVA.

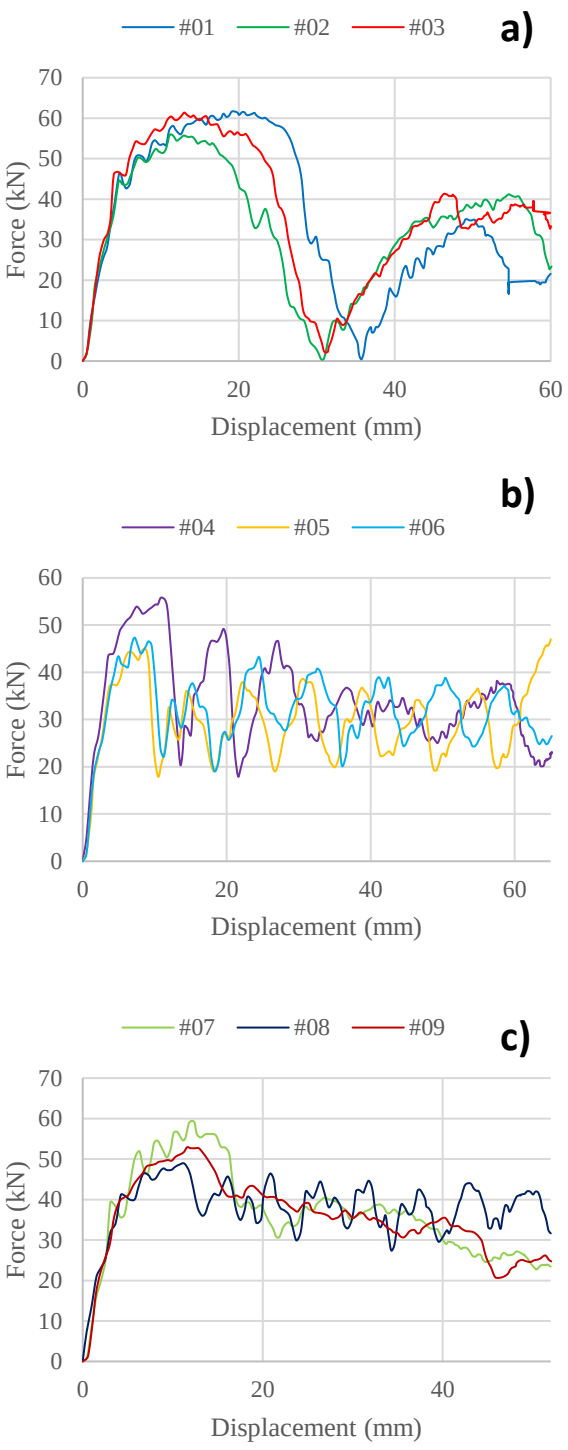


**Figure 4.** Force-displacement plots of; a) REC b) SC c) AH latticed sandwiches obtained by drop weight tests.

### 3.3. Optimization Study

Average S/N ratios and rankings of parameters are presented in Table 5. In this table, Delta states the difference between the maximum and minimum of the S/N ratio for each parameter. Rank is the order of parameters according to the energy absorption performance of cylindrical sandwich composites. It is seen from Table 5 that the lattice geometry is the most effective parameter on the energy absorption performance, while the shell thickness is the least effective parameter.

The S/N ratio variation of each factor that can be used to determine the optimum combination is shown in Figure 5. The level with the largest S/N ratio gives the optimum level of design factors. Therefore, in this study, the optimum combination was determined to be SC for lattice geometry, 1.2 mm for shell thickness, and 16 mm for core thickness. In addition to the optimum combination, the worst combination for specific energy absorption was determined to be AH for lattice geometry, 2.0 mm for shell thickness, and 24 mm for core thickness.

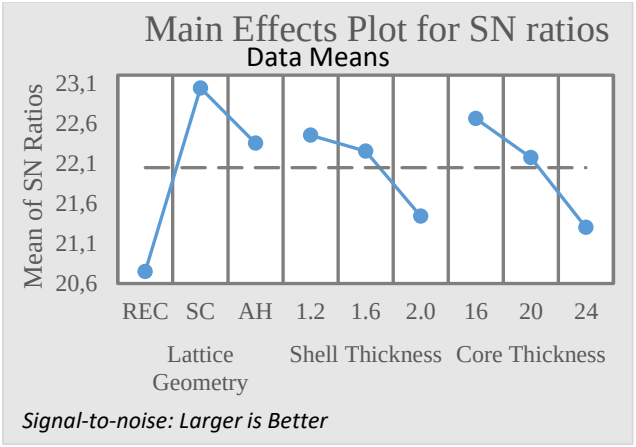


**Figure 5.** S/N ratios of the factors obtained by drop weight tests.

In addition to the Taguchi method, ANOVA has been used as a second method to support the reliability of the results. The level of each factor and specific energy absorption at these operating conditions are analysed by the ANOVA method, and the analysis results are given in Table 6. The calculated confidence level of the model was 93.44%. Lattice geometry was the most effective factor on specific energy absorption with a contribution ratio of 61.62%, and core thickness followed this parameter with a contribution ratio of 20.83%. Compared with these two factors, shell thickness had a slight effect on energy absorption, with a contribution ratio of 10.98%. These results show the same tendency as the results obtained from the Taguchi method.

**Table 4.** Results of the drop weight tests.

| Experiment | Level of Lattice Geometry | Level of Shell Thickness | Level of Core Thickness | Absorbed Energy (kJ) | SEA (J/g) | S/N Ratio |
|---|---|---|---|---|---|---|
| **#01** | 1 | 1 | 1 | 2.20 | 11.76 | 21.4070 |
| **#02** | 1 | 2 | 2 | 2.41 | 11.63 | 21.3084 |
| **#03** | 1 | 3 | 3 | 2.20 | 9.46 | 19.5200 |
| **#04** | 2 | 1 | 2 | 2.20 | 15.29 | 23.6872 |
| **#05** | 2 | 2 | 3 | 1.92 | 12.79 | 22.1384 |
| **#06** | 2 | 3 | 1 | 2.10 | 14.59 | 23.2832 |
| **#07** | 3 | 1 | 3 | 1.88 | 12.95 | 22.2438 |
| **#08** | 3 | 2 | 1 | 1.96 | 14.62 | 23.2965 |
| **#09** | 3 | 3 | 2 | 1.83 | 11.89 | 21.5042 |

**Table 5.** Average S/N ratios and ranking parameters

| Level | Lattice Geometry | Shell Thickness | Core Thickness |
|---|---|---|---|
| 1 | 20.75 | 22.45 | 22.66 |
| 2 | 23.04 | 22.25 | 22.17 |
| 3 | 22.35 | 21.44 | 21.3 |
| Delta (max-min) | 2.29 | 1.01 | 1.36 |
| Rank | 1 | 3 | 2 |

## 4. Conclusion and Suggestions

Applications of auxetic materials as energy absorbers are gaining increasing interest. To sum up, in this study, the energy absorption capability of the cylindrical sandwich consisting of an auxetic core and shells was examined. The auxetic parameters of materials were optimized to improve their energy absorption performance. The following is a conclusion of the major findings drawn from experiments and analysis:

- Force-displacement plots of SC and AH lattices had a range of peak forces well-balanced around a line. On the other hand, the REC lattice had a single peak force following the initial peak force. Force-displacement plots of SC and AH lattices showed the characteristic behaviour of energy absorbers, unlike REC.

- The Taguchi method optimized the lattice geometry, shell thickness, and core thickness for the highest energy absorption performance. S/N responses indicated that cylindrical sandwiches had the highest SEA

**Table 6.** ANOVA test results of the factors obtained by drop weight tests.

| Factor | DOF* | SS* | MS | F Value | P* (%) |
|---|---|---|---|---|---|
| Lattice Geometry | 2 | 16.733 | 8.3664 | 9.39 | 61.62 |
| Shell Thickness | 2 | 2.982 | 1.4908 | 1.67 | 10.98 |
| Core Thickness | 2 | 5.657 | 2.8285 | 3.18 | 20.83 |
| Error | 2 | 1.781 | 0.89 | | 6.56 |
| Total | 8 | 27.153 | | | 100 |

*DOF, Degree of Freedom; SS Sum of Square; P, Contribution

with a core thickness of 1.2 mm, a shell thickness of 16 mm, and a SC lattice.

- It was found that lattice geometry, which had a 61.62% rate of contribution, was the main factor affecting the energy absorption of the cylindrical sandwich by the ANOVA method.

As a result, this study can be a guide for researching new generation crash box design in the future. However, more studies are needed to evaluate crash performance beyond the energy absorption and correlate it with Poisson's ratios.

**Acknowledgment**

This work was supported by the Bursa Technical University Scientific Research Projects Coordination Unit (Project no: 220Y021) and TUBİTAK 2210-D program. We would like to thank Ermetal Automotive for their support in the supply of the 3D Printed specimens.

**Conflict of Interest Statement**

There is no conflict of interest between the authors.

**Statement of Research and Publication Ethics**

The study is complied with research and publication ethics.

**References**

[1] K. E. Evans and A. Alderson, "Auxetic materials: Functional materials and structures from lateral thinking!," *Advanced Materials*, vol. 12, no. 9, pp. 617–628, 2000, doi: 10.1002/(SICI)1521-4095(200005)12:9<617::AID-ADMA617>3.0.CO;2-3.

[2] G. N. Greaves, A. L. Greer, R. S. Lakes, and T. Rouxel, "Poisson's ratio and modern materials," *Nat Mater*, vol. 10, no. 11, pp. 823–837, 2011, doi: 10.1038/nmat3134.

[3] J. Zhang, G. Lu, and Z. You, "Large deformation and energy absorption of additively manufactured auxetic materials and structures: A review," *Compos B Eng*, vol. 201, no. 108340, pp. 1–36, 2020, doi: 10.1016/j.compositesb.2020.108340.

[4] A. Alomarah, S. H. Masood, and D. Ruan, "Out-of-plane and in-plane compression of additively manufactured auxetic structures," *Aerosp Sci Technol*, vol. 106, pp. 106–107, 2020, doi: 10.1016/j.ast.2020.106107.

[5] C. Luo, C. Z. Han, X. Y. Zhang, X. G. Zhang, X. Ren, and Y. M. Xie, "Design, manufacturing and applications of auxetic tubular structures: A review," *Thin-Walled Structures*, vol. 163, no. December 2020, 2021, doi: 10.1016/j.tws.2021.107682.

[6] Q. Gao, L. Wang, Z. Zhou, Z. D. Ma, C. Wang, and Y. Wang, "Theoretical, numerical and experimental analysis of three-dimensional double-V honeycomb," *Mater Des*, vol. 139, pp. 380–391, 2018, doi: 10.1016/j.matdes.2017.11.024.

[7] W. Lee *et al.*, "Effect of auxetic structures on crash behavior of cylindrical tube," *Compos Struct*, vol. 208, no. April 2018, pp. 836–846, 2019, doi: 10.1016/j.compstruct.2018.10.068.

[8] Y. Guo *et al.*, "Deformation behaviors and energy absorption of auxetic lattice cylindrical structures under axial crushing load," *Aerosp Sci Technol*, vol. 98, p. 105662, 2020, doi: 10.1016/j.ast.2019.105662.

[9] F. Usta, O. F. Ertaş, A. Ataalp, H. S. Türkmen, Z. Kazancı, and F. Scarpa, "Impact behavior of triggered and non-triggered crash tubes with auxetic lattices," *Multiscale and Multidisciplinary Modeling, Experiments and Design*, vol. 2, no. 2, pp. 119–127, 2019, doi: 10.1007/s41939-018-00040-z.

[10] H. Sun, C. Ge, Q. Gao, N. Qiu, and L. Wang, "Crashworthiness of sandwich cylinder filled with double-arrowed auxetic structures under axial impact loading," *International Journal of Crashworthiness*, pp. 1–10, 2021, doi: 10.1080/13588265.2021.1947071.

[11] X. Y. Zhang *et al.*, "A novel type of tubular structure with auxeticity both in radial direction and wall thickness," *Thin-Walled Structures*, vol. 163, no. March, p. 107758, 2021, doi: 10.1016/j.tws.2021.107758.

[12] L. Chen *et al.*, "Dynamic crushing behavior and energy absorption of graded lattice cylindrical structure under axial impact load," *Thin-Walled Structures*, vol. 127, no. October 2017, pp. 333–343, 2018, doi: 10.1016/j.tws.2017.10.048.

[13] L. Jiang and H. Hu, "Finite element modeling of multilayer orthogonal auxetic composites under low-velocity impact," *Materials*, vol. 10, no. 8, 2017, doi: 10.3390/ma10080908.

[14] B. G. Çakan, C. Ensarioglu, V. M. Küçükakarsu, I. E. Tekin, and M. Cemal Çakir, "Experimental and numerical investigation of in-plane and out-of-plane impact behaviour of auxetic honeycomb boxes produced by material extrusion," *Journal of the Faculty of Engineering and Architecture of Gazi University*, vol. 36, no. 3, pp. 1657–1667, 2021, doi: 10.17341/gazimmfd.829758.

[15] M. Cherief, A. Belaadi, M. Bouakba, M. Bourchak, and I. Meddour, "Behaviour of lignocellulosic fibre-reinforced cellular core under low-velocity impact loading: Taguchi method," *International Journal of Advanced Manufacturing Technology*, vol. 108, no. 1–2, pp. 223–233, 2020, doi: 10.1007/s00170-020-05393-9.

[16] Q. Gao, X. Zhao, C. Wang, L. Wang, and Z. Ma, "Multi-objective crashworthiness optimization for an auxetic cylindrical structure under axial impact loading," *Mater Des*, vol. 143, pp. 120–130, 2018, doi: 10.1016/j.matdes.2018.01.063.

[17] C. Qi, F. Jiang, C. Yu, and S. Yang, "In-plane crushing response of tetra-chiral honeycombs," *Int J Impact Eng*, vol. 130, no. April, pp. 247–265, 2019, doi: 10.1016/j.ijimpeng.2019.04.019.

[18] C. Qi *et al.*, "Quasi-static crushing behavior of novel re-entrant circular auxetic honeycombs," *Compos B Eng*, vol. 197, no. 108117, pp. 1–12, 2020, doi: 10.1016/j.compositesb.2020.108117.

[19] S. H. Ahn, M. Montero, D. Odell, S. Roundy, and P. K. Wright, "Anisotropic material properties of fused deposition modeling ABS," *Rapid Prototyp J*, vol. 8, no. 4, pp. 248–257, 2002, doi: 10.1108/13552540210441166.

[20] K. C. Ang, K. F. Leong, and C. K. Chua, "Investigation of the mechanical properties and porosity relationships in fused deposition modelling-fabricated porous structures," vol. 2, no. November 2005, pp. 100–105, 2006, doi: 10.1108/13552540610652447.

[21] O. A. Mohamed, S. H. Masood, and J. L. Bhowmik, "Optimization of fused deposition modeling process parameters : a review of current research and future prospects," pp. 42–53, 2015, doi: 10.1007/s40436-014-0097-7.

[22] G. Lu and T. Yu, "Introduction," *Energy Absorption of Structures and Materials*, pp. 68–87, 2003, doi: 10.1533/9781855738584.68.

[23] T. Shepherd, K. Winwood, P. Venkatraman, A. Alderson, and T. Allen, "Validation of a Finite Element Modeling Process for Auxetic Structures under Impact," *Phys Status Solidi B Basic Res*, vol. 257, no. 10, pp. 1–14, 2020, doi: 10.1002/pssb.201900197.

[24] A. H. Bademlioglu, A. S. Canbolat, N. Yamankaradeniz, and O. Kaynakli, "Investigation of parameters affecting Organic Rankine Cycle efficiency by using Taguchi and ANOVA methods," *Appl Therm Eng*, vol. 145, no. September, pp. 221–228, 2018, doi: 10.1016/j.applthermaleng.2018.09.032.

[25] F. Rayegani and G. C. Onwubolu, "Fused deposition modelling (fdm) process parameter prediction and optimization using group method for data handling (gmdh) and differential evolution (de)," *International Journal of Advanced Manufacturing Technology*, vol. 73, no. 1–4, pp. 509–519, 2014, doi: 10.1007/s00170-014-5835-2.